Synthesis and Antitumor Evaluation of Bis Aza-anthracene-9,10-diones and Bis Aza-anthrapyrazole-6-ones

Ippolito Antonini,*,[†] Giorgio Santoni,[‡] Roberta Lucciarini,[‡] Consuelo Amantini,[‡] Diego Dal Ben,[†] Rosaria Volpini,[†] and Gloria Cristalli[†]

Department of Chemical Sciences, University of Camerino, Via S. Agostino 1, 62032 Camerino, Italy, and Department of Experimental Medicine and Public Health, University of Camerino, Via Scalzino 3, 62032 Camerino, Italy

The good results obtained as potential antitumor drugs with aza-anthracenediones and aza-anthrapyrazoles, e.g. pixantrone, **1a**, and **1b** (Chart 1), prompted us to design and synthesize a series of symmetrical bis derivatives, compounds **7–10** (Chart 1). These compounds are dimers of different aza-anthracenedione and aza-anthrapyrazolone monomers connected by the linker found to be the most appropriate among potential bis intercalators synthesized by us. The DNA-binding properties of bis derivatives **7** and **8** have been examined using fluorometric techniques: these target compounds are excellent DNA ligands, with a clear binding site preference for AT-rich duplexes. In vitro cytotoxic activity of all target compounds **7–10** and of reference compound pixantrone toward human cancer adenocarcinoma cell line HT29 is also described. Two selected compounds have been investigated for their capacity of inducing early apoptosis.

Introduction

Among the synthetic anticancer drugs interacting with DNA, mitoxantrone (Chart 1) is one of the most used in mono as well as in combination therapy.[1–3] Although mitoxantrone has a better tolerance profile than doxorubicin, it is not devoid of significant toxic side effects, especially cardiotoxicity.[4] In the attempt to develop drugs with improved therapeutic properties, benzo-[*g*]isoquinoline-5,10-diones (aza-anthracenediones),[5] e.g., pixantrone (Chart 1), and indazolo[4,3-*gh*]isoquinoline-6-ones (aza-anthrapyrazoles),[6] e.g., **1a** and **1b** (BBR 3576 and BBR 3438, respectively, Chart 1), have been synthesized as mitoxantrone derivatives. These compounds show promising antitumor characteristics, in particular, against non-Hodgkin's lymphoma and leukemias, and pixantrone is currently in advanced clinical studies.[7] Moreover, mitoxantrone-induced apoptosis of B-cell chronic leukemia cells[8] and pixantrone induced-apoptosis of rat B lymphocytes in the course of experimental allergic encephalomyelitis (EAE)[9,a] have been reported.

We expected to enhance the biological properties of potential monointercalators, such as aza-anthracenediones and aza-anthrapyrazoles, by connecting two monomers with an appropriate linker to give bis derivatives, which generally present higher DNA affinity and prolonged drug residence time in DNA with respect to the monomer. On the basis of this rationale, positive results have been achieved with several potential symmetrical bisintercalating agents described in Chart 1: bis(benzoisoquinolines), e.g., **2**[10] and **3**[11] (LU 79553 and DMP 840, respectively), bis(imidazoacridines) e.g., **4**[12] (WMC-26), bis(acridine-4-carboxamides) **5**,[13] and bis(pyrimidoacridines) **6**.[14]

Thus, we designed a series of symmetrical bis derivatives, compounds **7–10** (Chart 1), in which different aza-anthracene-

dione and aza-anthrapyrazolone monomers are connected by the polyamine, found to be the most appropriate linker among bisintercalators synthesized by our research group.[13,14] In a more detailed manner, compounds **7** and **8** represent regioisomer bis derivatives of pixantrone, in which the linker connects the same benzo[*g*]isoquinoline-5,10-dione chromophore of pixantrone, in 9,9′ positions in the first case and in 6,6′ positions in the second case. Likewise for **7** and **8**, also compounds **9** and **10** are regioisomer derivatives, but their chromophores are different. Compounds **9** represent bis aza-anthrapyrazoles in which the indazolo[4,3-*gh*]isoquinolin-6-one chromophores, connected by the linker in 5,5′ positions, are the same as in **1** and **2**. Differently, compounds **10** represent bis derivatives of indazolo[3,4-*fg*]isoquinolin-6-one rings connected in 5,5′ positions, and their chromophores are different than those of **1** and **2**.

Chemistry

Schemes 1 and 2 show the synthetic pathways leading to the target derivatives **7–10**. According to Scheme 1, the 9-fluoro-5,10-dioxo-5,10-dihydrobenzo[*g*]isoquinolin-6-yl 4-methylbenzenesulfonate (**11a**)[6] was allowed to react with the bis(3-aminopropyl)methylamine in dry tetrahydrofuran (THF) in the presence of diisopropylethylamine at room temperature to afford the desired intermediate 9,9′-(3,3′-(methylazanediyl)bis(propane-3,1-diyl)bis(azanediyl))bis(5,10-dioxo-5,10-dihydrobenzo[*g*]isoquinoline-9,6-diyl) bis(4-methylbenzenesulfonate) (**12a**); in a similar way, **12b** and **12c** were obtained from **11b** and **11c**,[15] respectively. Target compounds **7a–7e** were obtained by the reaction at 100 °C of **12a** (**12b** for **7e**) with the suitable amine as the reagent/solvent. In the same manner, the final compounds **8a–8c** were yielded from **12c**.
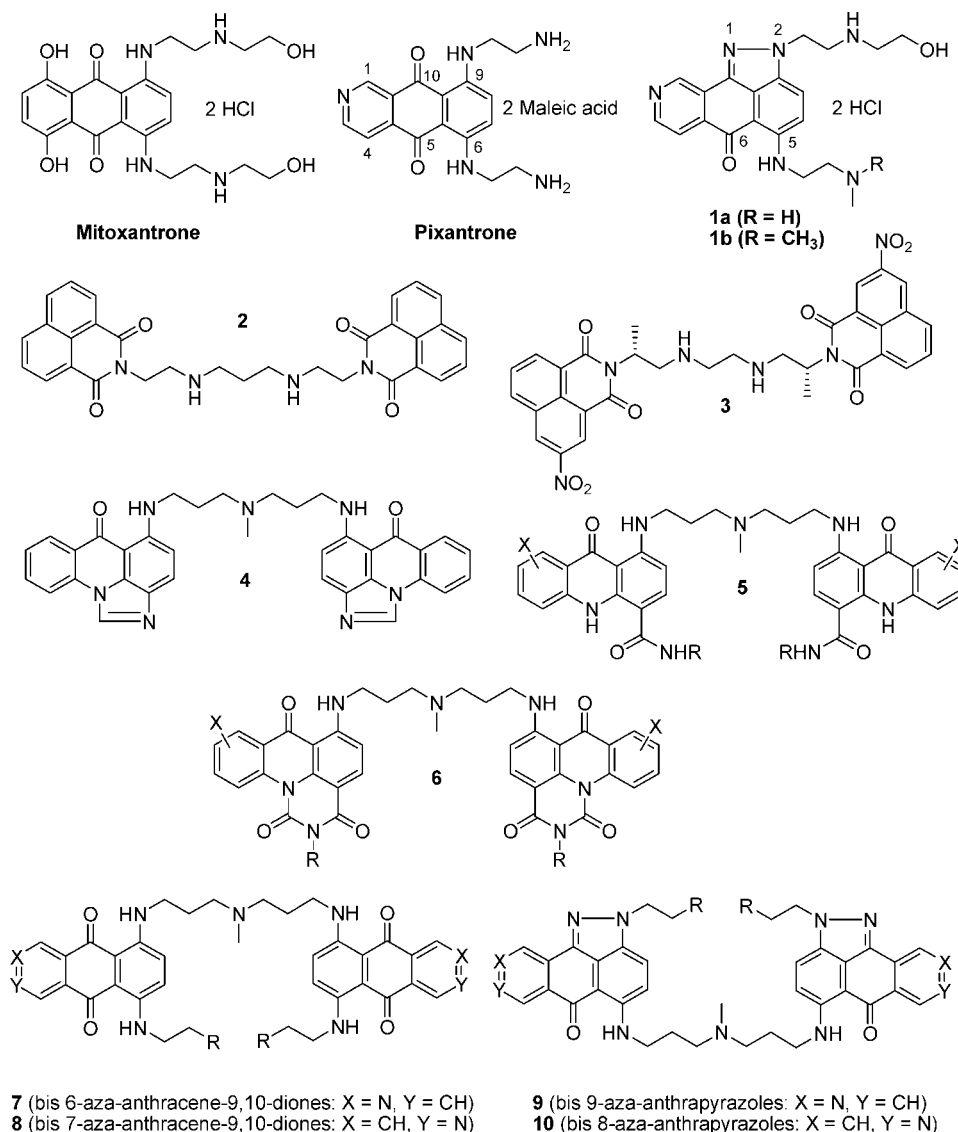
As shown in Scheme 2, the reaction of **11a** with the appropriate alkylaminoalkylhydrazine in THF in the presence of diisopropylethylamine at room temperature gave the intermediates **13a–13c**. In the same manner, **14a** and **14c** were obtained from **11d**[16] and **14b** from **11c**. Some of these intermediates (namely, **13a**, **13b**, and **14a**) have already been described.[6,16] Target compounds **9a–9c** and **10a–10c** were obtained by the reaction of the suitable intermediates **13a–13c**

* To whom correspondence should be addressed: Department of Chemical Sciences, University of Camerino, Via S. Agostino 1, I-62032 Camerino, Italy. Telephone: +39-0737-402235. Fax: +39-0737-637345. E-mail: ippolito.antonini@unicam.it.
    † Department of Chemical Sciences.
    ‡ Department of Experimental Medicine and Public Health.
    [a] Abbreviations: EAE, experimental allergic encephalomyelitis; CT-DNA, calf thymus DNA; AT, [poly(dA–dT)]$_2$; GC, [poly(dG–dC)]$_2$; Pix, pixantrone; AnnV, annexin V; PI, propidium iodide; PS, phosphatidylserine; DISC, death-inducing signalling complex; SRB, sulforhodamine B.

Chart 1. Structures of Mitoxantrone, Pixantrone, Compounds **1–6**, and Target Derivatives **7–10**

7 (bis 6-aza-anthracene-9,10-diones: X = N, Y = CH)
8 (bis 7-aza-anthracene-9,10-diones: X = CH, Y = N)

9 (bis 9-aza-anthrapyrazoles: X = N, Y = CH)
10 (bis 8-aza-anthrapyrazoles: X = CH, Y = N)

and **14a–14c**, respectively, with bis(3-aminopropyl)ethylamine in 2-ethoxyethanol in the presence of triethylamine at 120 °C.

Target compounds **7a–7e** and **8a–8c** were transformed in hydrochloride salts, while **9a–9c** and **10a–10c** were transformed in maleate salts, to obtain water-soluble compounds and estimate their DNA-binding and antineoplastic properties.

Results and Discussion

DNA-Binding Properties. As shown in Table 1, competitive displacement (C_{50}) fluorometric assays[17] with DNA-bound ethidium was used (a) to determine "apparent" equilibrium constants (K_{app}) for drug binding, because the C_{50} value is approximately inversely proportional to the binding constant,[18] and (b) to establish possible base- or sequence-preferential binding.[19] In the present study, fluorescence displacement assays were performed at pH 7 to enable a comparison under biological conditions. It was not possible to use this assay to determinate the C_{50} of target compounds **3** and **4** because of their own relevant fluorescence, which makes it impossible to follow the ethidium displacement by spectrofluorimetry.

In Table 1 are reported the K_{app} values, related to CT-DNA, AT, and GC, of the new derivatives **7** and **8**. The results indicate that target compounds **7** and **8** possess excellent DNA affinity,

greater or much greater than that of ethidium. Some conclusions can be drawn about the CT-DNA K_{app} values. (1) In the **7a–7e** subseries, it may be first evinced that **7a** is the strongest DNA binder among all tested derivatives and second that the nature of side chains in positions 6,6′ affects the DNA affinity in the K_{app} values range of 1.4–6.2 × 10^7. (2) In the **8a–8c** subseries, **8a** shows the highest K_{app} value but the range of variation (1.7–2.5 × 10^7) is narrower than that of corresponding regioisomers **7a–7c** (1.8–6.2 × 10^7). (3) The weak influence of regioisomery on DNA binding should be noted; in fact, there is not a very relevant difference between the subseries **7a–7c** and **8a–8c**. In any case, compounds **7** are always more DNA-affinic than corresponding compounds **8**.

Generally, the binding behavior of target compounds with synthetic polynucleotides does not parallel what we observed for CT-DNA (e.g., **8c** has the highest K_{app} values both versus AT and versus GC). However, it is important to emphasize the clear and, in some cases, very remarkable preference for binding to AT-rich duplexes.

Cytotoxic Activity. The human colon adenocarcinoma cell line (HT29) was used for cytotoxicity testing in vitro using the sulforhodamine B (SRB) assay.[20] In Table 1 are reported the in vitro cytotoxic activities of target bis derivatives **7–10** against

Scheme 1[a]
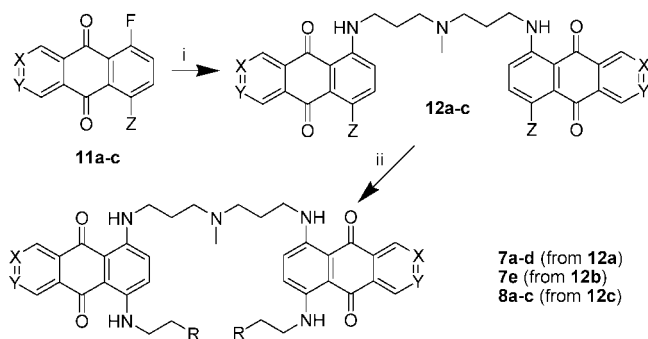
a Reagents and conditions: (i) bis(3-aminopropyl)ethylamine in dry THF in the presence of diisopropylethylamine, room temperature; (ii) the suitable amine as the reagent/solvent, 100 °C. Substituents: X = N and Y = CH for **11a**, **11b**, **12a**, **12b**, and **7**; X = CH and Y = N for **11c**, **12c**, and **8**; Z = OTs for **11a** and **12a**; Z = Cl for **11b**, **11c**, **12b**, and **12c**; R = N(CH₃)₂ for **7a** and **8a**, R = (CH₂)N(CH₃)₂ for **7b** and **8b**, R = N(C₂H₅)₂ for **7c** and **8c**, R = (CH₂)N(C₂H₅)₂ for **7d**, and R = 1-pyrrolidinyl for **7e**.

Scheme 2[a]
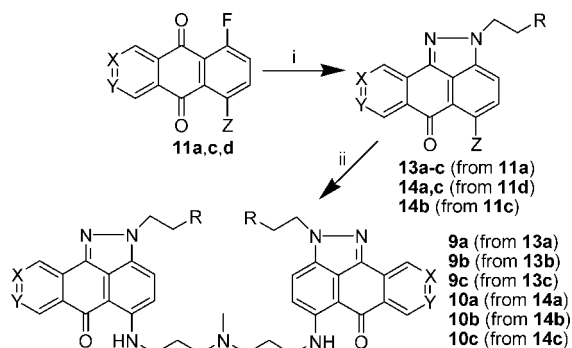
a Reagents and conditions: (i) the suitable alkylaminoalkylhydrazine in THF in the presence of *N*-ethyl-*N*-isopropylpropan-2-amine, room temperature; (ii) *N*-(3-aminopropyl)-*N*-methylpropane-1,3-diamine in 2-ethoxyethanol in the presence of triethylamine, 120 °C. Substituents: X = N and Y = CH for **11a**, **13a**−**13c**, and **9a**−**9c**; X = CH and Y = N for **11c**, **11d**, **14a**−**14c**, and **10a**−**10c**; Z = OTs for **11a**, **11d**, **13a**−**13c**, **14a**, and **14c**; Z = Cl for **11c** and **14b**; R = N(CH₃)₂ for **13a**, **14a**, **9a**, and **10a**, R = (CH₂)N(CH₃)₂ for **13b**, **14b**, **9b**, and **10b**, and R = N(C₂H₅)₂ for **13c**, **14c**, **9c**, and **10c**.

Table 1. DNA Binding and Cytotoxic Activity against Human Colon Adenocarcinoma (HT29) of Target Compounds **7**–**10**

compound	binding ($K_{app} \times 10^{-7}$ M⁻¹)[a]			cytotoxic activity[b]		
	AT[c]	CT-DNA	GC	GI₅₀	TGI	LC₅₀
7a	1.4 (2.5)	6.2	0.56	0.30	5.1	62
7b	2.9 (2.4)	3.8	1.2	2.0	7.9	>100
7c	1.9 (3.5)	1.8	0.55	4.5	32	>100
7d	2.0 (1.7)	1.4	1.2	83	>100	>100
7e	2.3 (2.4)	3.8	0.95	0.50	7.9	>100
8a	2.3 (7.7)	2.5	0.30	>100		
8b	1.9 (1.9)	1.7	1.0	>100		
8c	6.0 (5)	1.9	1.2	>100		
9a				0.00036	1.3	9.8
9b				1.6	>100	>100
9c				0.0010	4.5	97
10a				0.70	>100	>100
10b				40	>100	>100
10c				0.40	>100	>100
Pix				0.0012	3.2	100

a CT-DNA, AT, and GC refer to calf thymus DNA, [poly(dA−dT)]₂, and [poly(dG−dC)]₂, respectively. $K_{app} = 1.26/C_{50} \times 10^7$, in which 1.26 is the concentration (in micromolars) of ethidium in the ethidium−DNA complex, where C_{50} is the drug concentration (in micromolars) that effects a 50% drop in the fluorescence of bound ethidium, and 10^7 is the value of K_{app} assumed for ethidium in the complex. *b* Drug concentration (in micromolars) required to inhibit cell growth by 50% (GI₅₀) and 100% (TGI) or to kill 50% of the initial cell number (LC₅₀) after 72 h of drug exposure. Pix = Reference compound pixantrone. All assays were performed in triplicate. *c* In parentheses is the binding site preference, considered to be significant only for the [AT]/[GC] ratio, differing by >30% from the sequence-neutral unity value (i.e., <0.7 or >1.3).

of pentacyclic heterocyclic, shows GI₅₀ and TGI values similar to parent compound **7a** but seems devoid of cell killing capacity (LC₅₀ > 100 μM). (2) In the **8a**−**8c** subseries (**7a**−**7c** regioisomers), none of the new derivatives show any cytotoxic activity. However, this is not surprising because it has been reported that the position of the aza substitution on the anthracene nucleus is crucial for antineoplastic activity.[5] Differently from that found for DNA binding, the regioisomery plays a decisive role in the cytotoxic activity. (3) No simple correlation can be made between DNA binding and cytotoxic activity for either compounds **7** and, much more, compounds **8**. The only evident observation is that **7a** is the most CT-DNA-affinic compound and also the most cytotoxic among the bis pixantrone derivatives **7** and **8**. (4) Compounds **9a**−**9c** constitute the most potent of the four novel subseries. **9c** and particularly **9a** possess a very high capacity for cell growth inhibition (see the corresponding GI₅₀ and TGI values shown in Table 1). Moreover, **9a** also has cytocide activity in the low micromolar range. As in (1), the homologation of parent compound **9a** decreases the activity, but in this case, the lengthening of the distance between the two nitrogen atoms in the side chains (**9b**) produces a collapse in the activity, while more bulky substituents on the distal nitrogen atom of the side chains (**9c**) lead only to a small decrement of the activity. (5) Finally, the cytotoxic activity values of **10a**−**10c** subseries (**9a**−**9c** regioisomers) confirm the relevant effect of regioisomery: the position of the aza substitution on anthrapyrazole moiety is shown to highly influence cell growth inhibition and cytocide action (see also ref 6). However, in this case, the new derivatives preserve some inhibitory activity, especially **10c** and **10a**, but the TGI and LC₅₀ values are always >100 μM.

Apoptosis Assays. On the basis of their activity profiles and structure diversities, two compounds (**7a** and **9a**) were selected for further biological studies. Employing biparametric flow cytometric analysis using annexin V (AnnV) and propidium iodide (PI),[21] we analyzed whether treatment of HT29 cells with these antitumor agents would induce apoptotic and/or necrotic

HT29. Pixantrone was used as the reference compound. The results are expressed in terms of (i) growth inhibition 50, GI₅₀, (ii) total growth inhibition (TGI), which represent the drug concentration required to inhibit cell growth by 50 and 100%, respectively, and (iii) lethal concentration 50, LC₅₀, which represents the drug concentration required to kill 50% of the initial cell number. GI₅₀ gives an indication of the inhibitory action; TGI gives an indication of cytostatic action; and LC₅₀ gives an indication of the cytocide action of the drugs. Each quoted value is the mean of triplicate experiments. GI₅₀ values range from subnanomolar to >100 μM; the most active target compound appears to be **9a** (GI₅₀ value of 0.36 nM). Some derivatives show TGI values in the low micromolar range, and only three compounds demonstrate LC₅₀ values in the micromolar range. Overall, these data indicate that some target derivatives are potent inhibitors of HT29 cell growth, with two of them, **9a** and **9c**, being more potent than the reference compound pixantrone.

The following remarks can be made: (1) In the **7a**−**7e** subseries, considering **7a** as the parent compound, this is the most active compound, while the growing homologation of the side chains in 6,6′ positions leading to derivatives **7b**−**7d** result in a progressive decrement of antiproliferative activity. Compound **7e**, in which the distal nitrogen of the side chains is part

Table 2. Selected and Reference Compounds Induce PS Exposure in HT-29 Human Colon Adenocarcinoma Cells in a Time-Dependent Manner[a]

	PI⁻/AnnV⁻	PI⁺/AnnV⁻	PI⁻/AnnV⁺	PI⁺/AnnV⁺
		time: 6 h		
vehicle	92.2 ± 0.3	3.90 ± 0.2	2.60 ± 0.5	1.30 ± 0.7
7a	88.5 ± 0.9	3.30 ± 0.3	7.40 ± 1.0	0.80 ± 0.9
9a	72.5 ± 1.1	3.40 ± 0.8	22.3 ± 1.3	1.80 ± 0.3
Pix	60.4 ± 1.2	4.80 ± 0.7	32.5 ± 0.5	2.30 ± 1.1
		time: 12 h		
vehicle	91.0 ± 0.2	3.90 ± 0.2	2.60 ± 0.1	2.50 ± 0.2
7a	83.2 ± 1.8	5.30 ± 0.4	10.3 ± 0.9	1.20 ± 0.6
9a	60.0 ± 0.5	4.20 ± 0.9	32.4 ± 0.5	3.40 ± 0.7
Pix	50.4 ± 1.0	5.10 ± 1.1	38.4 ± 0.4	6.10 ± 0.4
		time: 24 h		
vehicle	82.0 ± 1.9	7.00 ± 0.6	3.90 ± 0.5	1.10 ± 0.5
7a	37.1 ± 0.9	8.30 ± 0.7	36.3 ± 1.3	18.3 ± 0.9
9a	8.30 ± 1.3	7.20 ± 1.2	62.3 ± 1.5	22.2 ± 1.1
Pix	41.6 ± 1.8	11.2 ± 1.1	41.0 ± 2.0	6.20 ± 0.7

[a] The apoptosis of HT29 cells treated at different times (6, 12, and 24 h) with the LC$_{50}$ concentration of the selected compounds and Pix was evaluated by biparametric cytofluorimetric analysis using PI and FITC-conjugated annexin V. Data expressed as the percentage of positive cells are the mean ± standard deviation (SD) of three separate experiments.

cell death. In fact, a characteristic feature of necrotic cell death is the loss of plasma membrane integrity. This damage can be highlighted by treatment with nonvital PI dye, which is allowed to penetrate into the cell, intercalating DNA, and turning it fluorescent. Instead, the exposure of phosphatidylserine (PS) represents an early and widespread hallmark of apoptotic cells. During the early phases of apoptosis, when the cell membrane remains intact, PS translocates from the inner to the outer layer of the plasma membrane. Thus, apoptotic cells may be evidenced by annexin V, which binds to negatively charged PS. Therefore, PI⁻/AnnV⁻ cells are living cells; PI⁺/AnnV⁻ cells are necrotic cells; PI⁻/AnnV⁺ cells are early apoptotic cells; and PI⁺/AnnV⁺ cells are late apoptotic or necrotic cells.

The results of biparametric flow cytometric analysis for the selected compounds and the reference compound pixantrone are reported in Table 2. Treatment with target compound **9a** induces a significant reduction (from 72.5 to 8.3%) of PI⁻/AnnV⁻ intact cells and early (6 h) translocation of PS in about 22.3% of the HT-29 cells (PI⁻/AnnV⁺). PS exposure of **9a**-treated HT-29 cells increases in a time-dependent manner, and about 62.3% of the HT-29 cells display PS 24 h after the treatment. Target compound **7a** also induces apoptosis, as proven by the increased percentage (from 3.7 to 36.3%) of PI⁻/AnnV⁺ HT-29 cells and the corresponding decrease (from 88.5 to 37.1%) of PI⁻/AnnV⁻ intact cells but in a less marked manner than **9a**. The reference compound pixantrone produces the highest (32.5% of the HT-29 cells PI⁻/AnnV⁺) very early (6 h) in the translocation of PS, but the percentage does not increase much more after 12−24 h. After 24 h, **9a** seems to be the most efficient apoptosis inducer among the three tested compounds. Neither apoptosis nor necrosis is observed in HT-29 cells treated with vehicle.

mRNA Expression Profiling of 7a and 9a Compound-Treated HT29 Cancer Cells. High-throughput mRNA expression profiling with a customized polymerase chain reaction (PCR) array was used as described in the Experimental Section.[22] Genes known to be involved in apoptotic cell death and DNA damage response were included in RT Profiler PCR Array Human Apoptosis. Untreated and **7a**- and **9a**-treated HT29 cells were plated at low density, and total RNA was isolated 6 and 12 h later. Consistent with the results presented in Tables 3 and 4, our findings demonstrate that in vitro

treatment with aza-antracenediones and aza-anthrapyrazolones derivates, namely, **7a** and **9a** compounds, inhibits growth and survival of HT29 human colon adenocarcinoma cells by affecting expression levels of multiple apoptosis-related genes. Of 84 defined apoptotic-related genes, 42 and 34 genes were affected by treatment with **7a** and **9a**, respectively. In particular, 28 of 42 genes (two-thirds) showing proapoptotic activity were upregulated (1 downregulated) by compound **7a**, whereas of 13 antiapoptotic genes, 4 are downregulated and 9 are upregulated by the same compound. Moreover, compound **9a** up- or downregulated the same number (16) of proapoptotic and antiapoptotic genes: among the proapoptotic genes, 5 are downregulated and 9 are upregulated, whereas among antiapoptotic genes, 14 are downregulated and 2 are upregulated.

Apoptosis can be initiated by extrinsic (death receptor) and intrinsic (mitochondrial) pathways (Figure 1).[23] In the extrinsic pathway, ligation of the death receptor induces the formation of a death-inducing signaling complex (DISC), composed of a death receptor (Fas or TNFRs), an adaptor protein (FADD and TRADD), and an initiator caspase (caspase 8). Clustering of death receptors promotes aggregation of procaspase 8 within DISC and induces autoproteolysis and generation of active caspase 8, further activating downstream effector caspase.[24] In the intrinsic pathway, the caspase cascade is initiated by mitochondrial depolarization and the release of proapoptotic factor. The apoptosome, a complex analogous to DISC, is formed when cytocrome *c* associates with APAF-1 and pro-caspase-9. Subsequently, caspase 9 is activated on the apoptosome and further activates downstream effector caspases.[25] Our findings indicate that the treatment of HT29 cancer cells with the aza-anthracenediones and aza-anthrapyrazolones derivates (**7a** and **9a**, respectively) affects genes representing multiple apoptosis-regulating pathways. Mitochondria-driven apoptosis pathways represent the mechanism by which **9a** induces apoptosis, whereas both death-receptor- and mitochondria-driven apoptotic mechanisms are activated by **7a**. In particular, **7a** but not **9a** upregulates death-receptor-associated apoptotic genes, including genes encoding death receptors themselves (FAS, DR5, CD27, and TNFRSF21), TNF ligands (CD70), adaptor proteins linking death receptors to intracellular apoptotic cascade (TRAF-2, TRAF-3, TRAF-4, FADD, and TRADD) and regulators of death receptor activity (CFAR and IAPs).[24,26] Another important gene affected by **7a** encodes for the P53 transcription factor, a stimulator of the production of several proapoptotic proteins. In addition, **7a** and **9a** enhanced the expression of several genes encoding members of the BCL-2 family of proteins (BID, BAD, BAX, BIK, BAK1, NIP1, NIP3, API3, ILP2, and BCL-2), which are involved in regulating the release of apoptosis-inducing factors from mitochondria.[25] Among the aforementioned genes, BID, induced by compound **7a** treatment, is of particular interest because it provides a link between death receptors and mitocondria-driven apoptotic pathways. The **7a**- and **9a**-treated HT29 cells displayed upregulation of the genes encoding major apoptosis-related caspases, including death-receptor-associated caspase 8 (**7a**), mitochondria-driven apoptosis-associated caspases 6 and 9 (**7a** and **9a**), and executioner caspase 7 (both compounds). Moreover, a gene encoding a substrate of apoptosis executioner caspase 3 (CIDE-B) along with the gene for caspase 3 inhibitor (NAIP) were upregulated by both compounds. Finally and very interestingly, compound **9a** markedly downregulated the expression of genes encoding members of the cell-survival cascade, such as AKT (AKT1), HSP70 (BAG1 and BAG4), BCL-2 (CIPER and MCL1), and IGFR1.[23] The strong downregulation (38 fold) of a type I

Table 3. Apoptosis-Related Genes Affected by **7a**-Treated HT-29 Human Colon Carcinoma Cells[a]

gene symbol	accession number	protein or gene	A/P[b]	fold change in HT-29 cells	
				6 h	12 h
CD70	NM_001252	CD70 molecule	P	2.2	2.2
FAS	NM_000043	Fas (TNF receptor superfamily, member 6)	P	2.2	
TNFRSF11B	NM_002546	tumor necrosis factor receptor superfamily, member 11b	P	2.1	
TNFRSF21	NM_014452	tumor necrosis factor receptor superfamily, member 21	P	3.7	
CD27	NM_001242	CD27 molecule	P	2.2	2.2
TRAF2	NM_021138	TNF receptor-associated factor 2	P	2.4	
TRAF3	NM_003300	TNF receptor-associated factor 3	P	4.5	
TRAF4	NM_004295	TNF receptor-associated factor 4	P	94	23
FADD	NM_003824	Fas (TNFRSF6)-associated via death domain	P	2.4	
TRADD	NM_003789	TNFRSF1A-associated via death domain	P	4.3	2.5
BAK1	NM_001188	BCL2-antagonist/killer 1	P	4.5	4.1
BAX	NM_004324	BCL2-associated X protein	P	5.3	3.0
BCL2L1	NM_138578	BCL2-like 1	A		−5.9
BCL2	NM_000633	B-cell CLL/lymphoma 2	A/P	4.2	7.8
BCL2L10	NM_020396	BCL2-like 10 (apoptosis facilitator)	A	3.1	3.0
BCL2L11	NM_006538	BCL2-like 11 (apoptosis facilitator)	P	7.7	
BCLAF1	NM_014739	BCL2-associated transcription factor 1	P		136
BID	NM_001196	BH3-interacting domain death agonist	P	4.3	
BIK	NM_001197	BCL2-interacting killer (apoptosis inducing)	P	5.2	
BNIP1	NM_001205	BCL2/adenovirus E1B 19 kDa interacting protein 1	P	3.0	
BNIP2	NM_004330	BCL2/adenovirus E1B 19 kDa interacting protein 2	A	−2.9	−3.3
BNIP3L	NM_004331	BCL2/adenovirus E1B 19 kDa interacting protein 3-like	P	7.4	3.6
MCL1	NM_021960	myeloid cell leukemia sequence 1 (BCL2-related)	A	−10	
CASP6	NM_032992	caspase 6, apoptosis-related cysteine peptidase	P	3.0	
CASP7	NM_001227	caspase 7, apoptosis-related cysteine peptidase	P	6.4	3.0
CASP8	NM_001228	caspase 8, apoptosis-related cysteine peptidase	P	2.5	
CASP9	NM_001229	caspase 9, apoptosis-related cysteine peptidase	P	3.0	8.5
CFLAR	NM_003879	CASP8 and FADD-like apoptosis regulator	A	4.0	
NOD1	NM_006092	nucleotide-binding oligomerization domain containing 1	P	4.2	
CARD6	NM_032587	caspase recruitment domain family, member 6	A/P	−5.0	
CARD8	NM_014959	caspase recruitment domain family, member 8	P	4.0	
CIDEB	NM_014430	cell-death-inducing DFFA-like effector b	P	9.3	4.4
NOL3	NM_003946	nucleolar protein 3 (apoptosis repressor with CARD domain)	A	4.7	15
ABL1	NM_005157	V-abl Abelson murine leukemia viral oncogene homologue 1	A	33	58
GADD45A	NM_001924	growth arrest and DNA-damage-inducible, α	A	3.0	
TP53	NM_000546	tumor protein p53 (Li−Fraumeni syndrome)	A/P	3.0	
BFAR	NM_016561	bifunctional apoptosis regulator	A/P	5.4	−2.5
BRAF	NM_004333	V-raf murine sarcoma viral oncogene homologue B1	A	2.4	
NAIP	NM_004536	NLR family, apoptosis inhibitory protein	A	9.6	52
BIRC3	NM_001165	baculoviral IAP repeat-containing 3	A	2.5	
BIRC4	NM_001167	baculoviral IAP repeat-containing 4	A	9.3	2.0
BIRC8	NM_033341	baculoviral IAP repeat-containing 8	A	−2.3	

[a] Gene included are 2-fold or greater up- or downregulated. A fold change greater than 3 has a confidence interval of 99%, and a fold change greater than 2 has a confidence interval of 90%. Messenger RNA levels were normalized to β-actin levels by the $\Delta\Delta$Ct method and are expressed as a fold increase in HT-29 cells. The mean of three biological repeats with a similar general fold increase is presented. [b] A = antiapoptotic genes and P = proapoptotic genes. A/P genes may act as anti or pro and have been considered among the proapoptotic ones in the present context.

insulin-like growth factor receptor gene induced by **9a** is particularly relevant in HT29 cancer cells. Insulin-like growth factor receptor is overexpressed in colon carcinomas and mediates proliferation, motility, and survival; moreover, silencing of the IGFR1 gene is associated with an increased susceptibility of cancer cells to mitoxantrone, etoposide, and ionizing radiation.[27] Thus, mitochondria-driven apoptosis represents a major mechanism of **9a**-mediated cell death, whereas both death-receptor- (primarily) and mitochondria (secondarily) driven apoptotic pathways were activated by compound **7a** (Figure 1). The early and better cytotoxic activity shown by **9a**, with respect to **7a**, may be the result of a marked upregulation of proapoptotic genes and the combined downregulation of survival genes, which sensitize HT29 colon carcinoma cells to apoptotic stimuli.

Conclusions

The present study led to the discovery of two subseries of compounds, namely, derivatives **7** and **9**, which demonstrate intriguing anticancer properties. The selected compounds **7a** and **9a** may be considered new leads in the field of anticancer

derivatives. In particular, compound **9a**, which shows very potent cytostatic and cytocide action and a high capacity for early apoptosis induction, may be a good candidate for in vivo preclinical studies. Moreover, its marked upregulation of proapoptotic genes, particularly combined with the downregulation of survival genes that sensitizes tumor cells to chemotherapy, may make **9a** useful in combination therapies.

Experimental Section

Synthetic Chemistry. Melting points were determined on a Büchi 540 apparatus and are uncorrected. Thin-layer chromatography (TLC) was accomplished using plates precoated with silica gel 60 F-254 (Merck). All ^{1}H nuclear magnetic resonance (NMR) spectra were recorded on a Varian VXR 300 instrument. Chemical shifts are reported as δ values (ppm) downfield from internal Me$_4$Si in the solvent shown. The following NMR abbreviations are used: br (broad), s (singlet), d (doublet), t (triplet), q (quadruplet), m (multiplet), ar (aromatic proton), and ex (exchangeable with D$_2$O). Elemental analyses were performed on an EA1108CHAZ-O elemental analyzer (Fisons Instruments).

1,9-Bis{9-[(5,10-dioxo-5,10-dihydrobenzo[*g*]isoquinoline-6-yl) tosylate]yl}-5-methyl-1,5,9-triazanonane (12a). Example of the

Table 4. Apoptosis-Related Genes Affected by **9a**-Treated HT29 Human Colon Carcinoma Cells[a]

gene symbol	accession number	protein or gene	A/P[b]	fold change in HT-29 cells	
				6 h	12 h
LTBR	NM_002342	lymphotoxin β receptor (TNFR superfamily, member 3)	P	−5.3	−4.3
TNFRSF10A	NM_003844	tumor necrosis factor receptor superfamily, member 10a	A/P	−2.5	−5.9
TNFRSF10B	NM_003842	tumor necrosis factor receptor superfamily, member 10b	A/P		−4.3
BAX	NM_004324	BCL2-associated X protein	P	4.1	1.3
BAK1	NM_001188	BCL2-antagonist/killer 1	P	4.5	4.1
BAG1	NM_004323	BCL2-associated athanogene	A	−2.5	
BAG4	NM_004874	BCL2-associated athanogene 4	A	−7.0	−3.3
BCL2L1	NM_138578	BCL2-like 1	A	1.2	
BCL2	NM_000633	B-cell CLL/lymphoma 2	A/P	−2.8	
BCL2L10	NM_020396	BCL2-like 10 (apoptosis facilitator)	A	2.2	
BCL10	NM_003921	B-cell CLL/lymphoma 10	A		−2.2
BCL2L11	NM_006538	BCL2-like 11 (apoptosis facilitator)	P	7.7	
BCLAF1	NM_014739	BCL2-associated transcription factor 1	P		136
BNIP1	NM_001205	BCL2/adenovirus E1B 19 kDa interacting protein 1	P	3.0	
BNIP3L	NM_004331	BCL2/adenovirus E1B 19 kDa interacting protein 3-like	P	7.4	3.6
MCL1	NM_021960	myeloid cell leukemia sequence 1 (BCL2-related)	A	−5.0	−2.7
CASP7	NM_001227	caspase 7, apoptosis-related cysteine peptidase	P	5.6	
CASP9	NM_001229	caspase 9, apoptosis-related cysteine peptidase	P	2.2	
NOD1	NM_006092	nucleotide-binding oligomerization domain containing 1	P	4.2	
CARD6	NM_032587	caspase recruitment domain family, member 6	P	−2.7	−6.7
CARD8	NM_014959	caspase recruitment domain family, member 8	P	4.0	
CIDEB	NM_014430	cell-death-inducing DFFA-like effector b	P	8.3	2.4
CFLAR	NM_003879	CASP8 and FADD-like apoptosis regulator	A	−2.2	−3.3
NOL3	NM_003946	nucleolar protein 3 (apoptosis repressor with CARD domain)	A	−2.5	−3.8
AKT1	NM_005163	V-akt murine thymoma viral oncogene homologue 1	A		−6.3
GADD45A	NM_001924	growth arrest and DNA-damage-inducible, α	A	8.8	
BFAR	NM_016561	bifunctional apoptosis regulator	A	−7.0	−2.5
BRAF	NM_004333	V-raf murine sarcoma viral oncogene homologue B1	A		−9.1
IGF1R	NM_000875	insulin-like growth factor 1 receptor	A	−38.5	−4.0
BIRC3	NM_001165	baculoviral IAP repeat-containing 3	A		−6.3
BIRC6	NM_016252	baculoviral IAP repeat-containing 6 (apollon)	A	−2.6	
BIRC8	NM_033341	baculoviral IAP repeat-containing 8	A	−5.6	−33.3

[a] Gene included are 2-fold or greater up- or downregulated. A fold change greater than 3 has a confidence interval of 99%, and a fold change greater than 2 has a confidence interval of 90%. Messenger RNA levels were normalized to β-actin levels by the $\Delta\Delta Ct$ method and are expressed as a fold increase in HT-29 cells. The mean of three biological repeats with a similar general fold increase is presented. [b] A = antiapoptotic genes and P = proapoptotic genes. A/P genes may act as anti or pro and have been considered among the proapoptotic ones in the present context.

General Procedure for the Preparation of 12a−12c. A solution of bis(3-aminopropyl)ethylamine (0.05 mL, 0.25 mmol) in dry THF (1.5 mL) was added dropwise to a solution of 9-fluoro-5,10-dioxo-5,10-dihydrobenzo[g]isoquinolin-6-yl tosylate (**11a**; 0.2 g, 0.5 mmol) in dry THF (2 mL) in the presence of diisopropylethylamine (0.1 mL, 0.5 mmol). The resulting mixture was stirred at room temperature for 3 h and then partitioned between CHCl$_3$ (30 mL) and an excess of 1 M aqueous Na$_2$CO$_3$ (2 × 30 mL). The organic layer was worked up to give a residue that was purified by flash chromatography on a silica gel column eluted with CHCl$_3$/MeOH (95:1, v/v) to obtain **12a** as a red solid used as such for the next step. Yield 25%. mp 140–142 °C. ^{1}H NMR (CDCl$_3$) δ: 1.92 (m, 4H, 2 × CH$_2$), 2.30 (s, 3H, N-CH$_3$), 2.38 (s, 6H, 2 × CH$_3$), 2.57 (t, 4H, 2 × CH$_2$), 3.40 (m, 4H, 2 × CH$_2$), 7.02 (d, 2H, ar), 7.29 (d, 8H, ar), 7.72 (d, 2H, ar), 7.83 (d, 2H, ar), 8.90 (d, 2H, ar), 9.38 (s, 2H, ar), 10.05 (t, 2H, 2 × NH, ex).

The intermediate derivatives **12b** and **12c** were prepared in a similar manner from **11b** and **11c**.

1,9-Bis{6-[2-(dimethylamino)ethylamino]-5,10-dioxo-5,10-dihydrobenzo[g]isoquinoline-9-yl}-5-methyl-1,5,9-triazanonane (7a). Example of the General Procedure for the Preparation of 7a−7e and 8a−8c. A solution of **12a** (0.1 g, 0.11 mmol) in 2-dimethylaminoethylamine (2 mL) was stirred at 100 °C for 2 h and then partitioned between CHCl$_3$ (30 mL) and an excess of 1 M aqueous Na$_2$CO$_3$ (2 × 30 mL). The organic layer was worked up to give a residue that was purified by flash chromatography on a silica gel column eluted with CHCl$_3$/MeOH (1:1, v/v) and 32% aqueous NH$_3$ (10 mL for 1 L of eluent) to give pure **7a** (0.02 g, yield 25%), which was directly converted in hydrochloride salt by the usual methods. Hydrochloride mp 140–142 °C. ^{1}H NMR (CDCl$_3$) δ: 1.92 (m, 4H, 2 × CH$_2$), 2.25–2.40 (m, 15H, 5 × CH$_3$), 2.52–2.69 (m, 8H, 4 × CH$_2$), 3.32–3.56 (m, 8H, 4 × CH$_2$), 7.03 (d, 2H, ar), 7.18 (d, 2H, ar), 8.05 (d, 2H, ar), 8.85 (d, 2H, ar), 9.48 (s, 2H, ar), 10.88–11.07 (m, 4H, 4 × NH, ex). Anal. Calcd (C$_{41}$H$_{49}$N$_9$O$_4$) C, H, N.

The final compounds **7b−7d** (from **12a**), **7e** (from **12b**), and **8a−8c** (from **12c**) were prepared in the same experimental conditions using the appropriate alkylaminoalkylamine. All of the target compounds were converted to water-soluble hydrochloride salts by the usual methods.

Data for 1,9-Bis{6-[3-(dimethylamino)propylamino]-5,10-dioxo-5,10-dihydrobenzo[g]isoquinoline-9-yl}-5-methyl-1,5,9-triazanonane (7b). Yield 71%. mp 126–128 °C. Hydrochloride mp 175–177 °C (EtOH). ^{1}H NMR (CDCl$_3$) δ: 1.67–2.00 (m, 8H, 4 × CH$_2$), 2.22 (s, 12H, 4 × CH$_3$), 2.30 (s, 3H, 5-CH$_3$), 2.40 (t, 4H, 2 × CH$_2$), 2.59 (t, 4H, 2 × CH$_2$), 3.30–3.52 (m, 8H, 4 × CH$_2$), 7.00–7.18 (m, 4H, ar), 7.97 (d, 2H, ar), 8.82 (d, 2H, ar), 9.48 (s, 2H, ar), 10.83–11.07 (m, 4H, 4 × NH, ex). Anal. Calcd (C$_{43}$H$_{53}$N$_9$O$_4$) C, H, N.

Data for 1,9-Bis{6-[2-(diethylamino)ethylamino]-5,10-dioxo-5,10-dihydrobenzo[g]isoquinoline-9-yl}-5-methyl-1,5,9-triaza-nonane (7c). Yield 60%. mp 107–109 °C. Hydrochloride mp 172–173 °C (EtOH). ^{1}H NMR (CDCl$_3$) δ: 1.09 (t, 12H, 4 × CH$_3$), 1.94 (m, 4H, 2 × CH$_2$), 2.31 (s, 3H, 5-CH$_3$), 2.51–2.70 (m, 12H, 6 × CH$_2$), 2.78 (t, 4H, 2 × CH$_2$), 3.32–3.52 (m, 8H, 4 × CH$_2$), 7.01–7.18 (m, 4H, ar), 8.03 (d, 2H, ar), 8.85 (d, 2H, ar), 9.50 (s, 2H, ar), 10.86–11.03 (m, 4H, 4 × NH, ex). Anal. Calcd (C$_{45}$H$_{57}$N$_9$O$_4$) C, H, N.

Data for 1,9-Bis{6-[3-(diethylamino)propylamino]-5,10-dioxo-5,10-dihydrobenzo[g]isoquinoline-9-yl}-5-methyl-1,5,9-triaza-nonane (7d). Yield 35%. mp 82–84 °C. Hydrochloride mp 186–188 °C (EtOH). ^{1}H NMR (CDCl$_3$) δ: 1.05 (t, 12H, 4 × CH$_3$), 1.82–2.02 (m, 8H, 4 × CH$_2$), 2.31 (s, 3H, 5-CH$_3$), 2.52–2.66 (m, 16H, 8 × CH$_2$), 3.32–3.50 (m, 8H, 4 × CH$_2$), 7.03–7.18 (m, 4H, ar), 7.97 (d, 2H, ar), 8.84 (d, 2H, ar), 9.45 (s, 2H, ar), 10.87–11.02 (m, 4H, 4 × NH, ex). Anal. Calcd (C$_{47}$H$_{61}$N$_9$O$_4$) C, H, N.
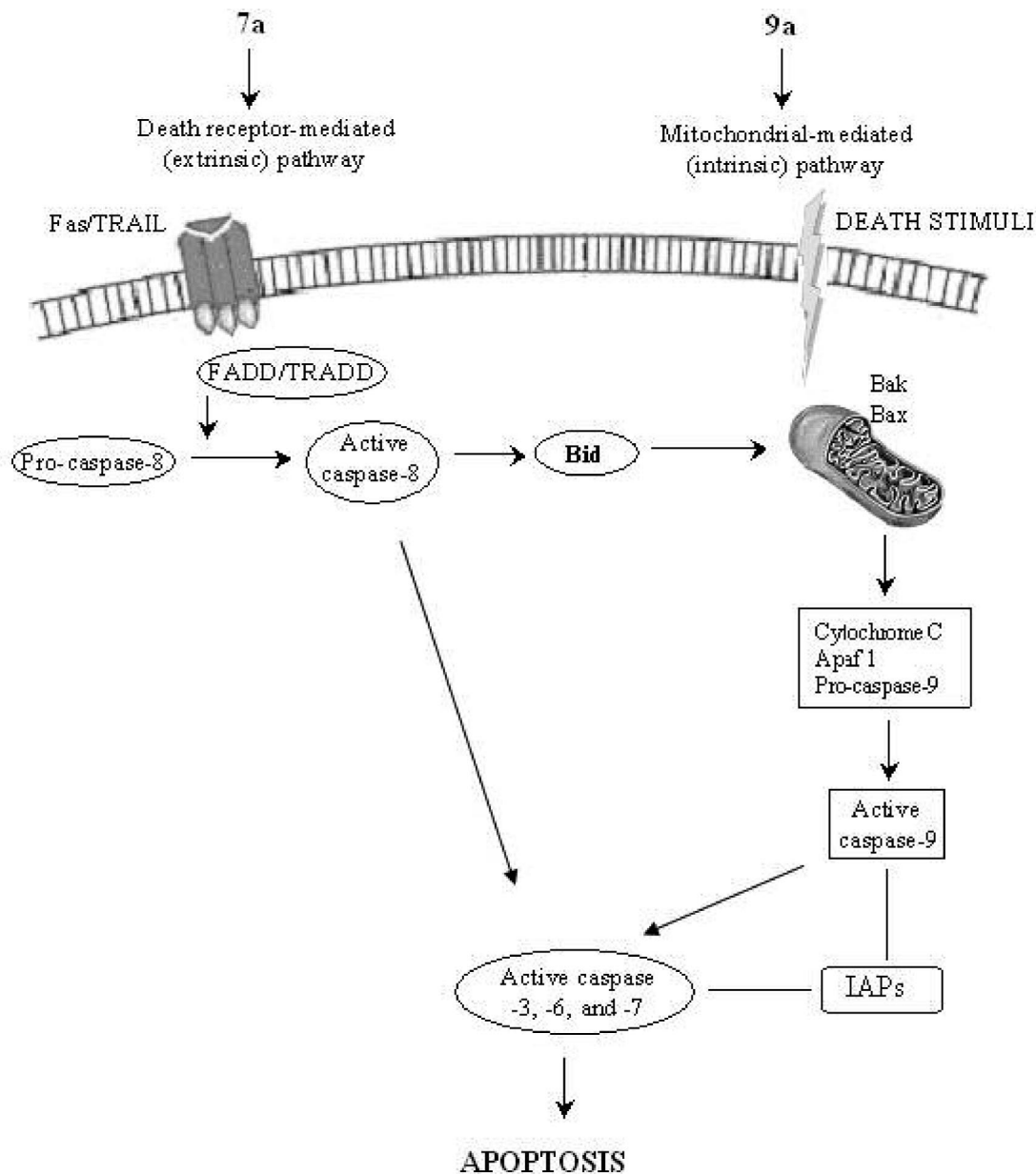
Figure 1. Apoptosis pathways.

Data for 1,9-Bis{6-[2-(1-pyrrolidinyl)ethylamino]-5,10-dioxo-5,10-dihydrobenzo[*g*]isoquinoline-9-yl}-5-methyl-1,5,9-triaza-nonane (7e). Yield 40%. Hydrochloride mp >250 °C (EtOH). ^{1}H NMR (CDCl$_3$) δ: 1.80 (m, 8H, 4 × CH$_2$), 1.92 (m, 4H, 2 × CH$_2$), 2.29 (s, 3H, CH$_3$), 2.60 (m, 12H, 6 × CH$_2$), 2.79 (t, 4H, 2 × CH$_2$), 3.37–3.52 (m, 8H, 4 × CH$_2$), 7.02 (d, 2H, ar), 7.16 (d, 2H, ar), 7.98 (d, 2H, ar), 8.82 (d, 2H, ar), 9.45 (s, 2H, ar), 10.90 (t, 2H, 2 × NH, ex), 10.99 (t, 2H, 2 × NH, ex). Anal. Calcd (C$_{45}$H$_{53}$N$_9$O$_4$) C, H, N.

Data for 1,9-Bis{9-[2-(dimethylamino)ethylamino]-5,10-dioxo-5,10-dihydrobenzo[*g*]isoquinoline-6-yl}-5-methyl-1,5,9-triaza-nonane (8a). Yield 31%. mp 158–160 °C. Hydrochloride mp 204–205 °C (EtOH). ^{1}H NMR (CDCl$_3$) δ: 1.94 (m, 4H, 2 × CH$_2$), 2.34 (s, 3H, 5-CH$_3$), 2.42 (s, 12H, 4 × CH$_3$), 2.62 (t, 4H, 2 × CH$_2$), 2.71 (t, 4H, 2 × CH$_2$), 3.40–3.51 (m, 8H, 4 × CH$_2$), 7.00–7.11 (m, 4H, ar), 7.97 (d, 2H, ar), 8.81 (d, 2H, ar), 9.50 (s, 2H, ar), 10.85 (t, 2H, 2 × NH, ex), 10.96 (t, 2H, 2 × NH, ex). Anal. Calcd (C$_{41}$H$_{49}$N$_9$O$_4$) C, H, N.

Data for 1,9-Bis{9-[3-(dimethylamino)propylamino]-5,10-di-oxo-5,10-dihydrobenzo[*g*]isoquinoline-6-yl}-5-methyl-1,5,9-tri-azanonane (8b). Yield 61%. mp 125–126 °C. Hydrochloride mp 150–151 °C (EtOH). ^{1}H NMR (CDCl$_3$) δ: 1.80–2.00 (m, 8H, 4 × CH$_2$), 2.23 (s, 12H, 4 × CH$_3$), 2.30 (s, 3H, 5-CH$_3$), 2.40 (t, 4H, 2 × CH$_2$), 2.59 (t, 4H, 2 × CH$_2$), 3.30–3.50 (m, 8H, 4 × CH$_2$), 7.05–7.15 (m, 4H, ar), 7.99 (d, 2H, ar), 8.82 (d, 2H, ar), 9.52 (s, 2H, ar), 10.90 (t, 2H, 2 × NH, ex), 11.03 (t, 2H, 2 × NH, ex). Anal. Calcd (C$_{43}$H$_{53}$N$_9$O$_4$) C, H, N.

Data for 1,9-Bis{9-[2-(diethylamino)ethylamino]-5,10-dioxo-5,10-dihydrobenzo[*g*]isoquinoline-6-yl}-5-methyl-1,5,9-triaza-nonane (8c). Yield 30%. mp 148–150 °C. Hydrochloride mp 165–168 °C (EtOH). ^{1}H NMR (CDCl$_3$) δ: 1.10 (t, 12H, 4 × CH$_3$), 1.98 (m, 4H, 2 × CH$_2$), 2.33 (s, 3H, 5-CH$_3$), 2.55–2.72 (m, 12H, 6 × CH$_2$), 2.79 (t, 4H, 2 × CH$_2$), 3.38–3.58 (m, 8H, 4 × CH$_2$), 7.02–7.22 (m, 4H, ar), 7.98–8.10 (m, 2H, ar), 7.82–8.90 (m, 2H, ar), 9.58 (s, 2H, ar), 10.90–11.11 (m, 4H, 4 × NH, ex). Anal. Calcd (C$_{45}$H$_{57}$N$_9$O$_4$) C, H, N.

2-(2-(Diethylamino)ethyl)-6-oxo-2,6-dihydroindazolo[4,3-*gh*]iso-quinolin-5-yl 4-Methylbenzenesulfonate (13c). Example of the General Procedure for the Preparation of 13a−13c and 14a−14c. A solution of 2-diethylaminoethylhydrazine (0.39 g, 3.0 mmol) in dry THF (1 mL) was added dropwise to a solution of 9-fluoro-5,10-dioxo-5,10-dihydrobenzo[*g*]isoquinolin-6-yl tosylate (**11a**; 0.4 g, 1 mmol) in dry THF (2 mL) in the presence of diisopropylethylamine (0.2 mL, 1.1 mmol). The resulting mixture

was stirred at room temperature for 1 h and then partitioned between CHCl₃ (30 mL) and an excess of 1 M aqueous Na₂CO₃ (2 × 30 mL). The organic layer was worked up to give a residue that was purified by flash chromatography on a silica gel column eluted with CHCl₃/MeOH (30:1, v/v) to obtain **13c** as a solid used as such for the next step. Yield 45%. mp 135–137 °C. ¹H NMR (CDCl₃) δ: 0.92 (t, 6H, 2 × CH₃), 2.44 (s, 3H, CH₃), 2.56 (q, 4H, 2 × CH₂), 3.01 (t, 2H, CH₂), 4.57 (t, 2H, CH₂), 7.28–7.40 (m, 2H, ar), 7.53 (d, 1H, ar), 7.81 (d, 1H, ar), 7.91–8.02 (m, 2H, ar), 8.08 (d, 1H, ar), 8.82 (d, 1H, ar), 9.55 (s, 1H, ar).

The intermediate derivatives **13a**, **13b**, and **14a–14c** were prepared in a similar manner from **11a**, **11d**, and **11c**.

1,9-Bis{2-[2-(dimethylamino)ethyl]-6-oxo-2,6-dihydroindazolo[4,3-*gh*]isoquinolin-5-yl}-5-methyl-1,5,9-triazanonane (9a). Example of the General Procedure for the Preparation of 9a–9c and 10a–10c. A solution of bis(3-aminopropyl)ethylamine (0.035 mL, 0.19 mmol) and **13a** (0.18 g, 0.39 mmol) in 2-ethoxyethanol (5 mL) and triethylamine (0.5 mL) were heated at 120 °C for 5 h under stirring. The resulting mixture was partitioned between CHCl₃ (30 mL) and an excess of 1 M aqueous Na₂CO₃ (2 × 30 mL). The organic layer was worked up to give a residue that was purified by flash chromatography on a silica gel column eluted first with CHCl₃/MeOH (1:1 v/v) and then with CHCl₃/MeOH (1:1 v/v) containing 32% aqueous NH₃ (50 mL for 1 L of eluent) to obtain **9a**. Yield 29%. mp 85–86 °C. ¹H NMR (CDCl₃) δ: 1.99 (m, 4H, 2 × CH₂), 2.32 (s, 12H, 4 × CH₃), 2.37 (s, 3H, 5-CH₃), 2.63 (t, 4H, 2 × CH₂), 2.88 (t, 4H, 2 × CH₂), 3.52 (m, 4H, 2 × CH₂), 4.48 (t, 4H, 2 × CH₂), 6.77 (d, 2H, ar), 7.34 (d, 2H, ar), 8.23 (d, 2H, ar), 8.72 (d, 2H, ar), 9.20 (t, 2H, 2 × NH, ex), 9.60 (s, 2H, ar). Anal. Calcd (C₄₁H₄₇N₁₁O₂) C, H, N.

The target compounds **9b**, **9c**, and **10a–10c** were prepared in the same experimental conditions from **13b**, **13c**, and **14a–14c**, respectively. All of the target compounds were converted to water-soluble dimaleate salts by usual methods.[6]

Data for 1,9-Bis{2-[3-(dimethylamino)propyl]-6-oxo-2,6-dihydroindazolo[4,3-*gh*]isoquinolin-5-yl}-5-methyl-1,5,9-triazanonane (9b). Yield 20%. Dimaleate mp 115–116 °C. ¹H NMR (DMSO-d₆) δ: 1.98–2.21 (m, 4H, 2 × CH₂), 2.42 (s, 12H, 4 × CH₃), 2.51 (s, 3H, 5-CH₃), 2.59 (t, 4H, 2 × CH₂), 2.78 (t, 4H, 2 × CH₂), 3.44–3.63 (m, 8H, 4 × CH₂), 4.45 (t, 4H, 2 × CH₂), 6.77 (d, 2H, ar), 7.37 (d, 2H, ar), 8.23 (d, 2H, ar), 8.75 (d, 2H, ar), 9.22 (t, 2H, 2 × NH, ex), 9.60 (s, 2H, ar). Anal. Calcd (C₄₃H₅₁N₁₁O₂) C, H, N.

Data for 1,9-Bis{2-[2-(diethylamino)ethyl]-6-oxo-2,6-dihydroindazolo[4,3-*gh*]isoquinolin-5-yl}-5-methyl-1,5,9-triazanonane (9c). Yield 30%. Dimaleate mp 109–110 °C. ¹H NMR (CDCl₃) δ: 0.95 (t, 12H, 4 × CH₃), 1.97 (m, 4H, 2 × CH₂), 2.35 (s, 3H, 5-CH₃), 2.47–2.58 (m, 8H, 4 × CH₂), 2.61 (t, 4H, 2 × CH₂), 2.85 (t, 4H, 2 × CH₂), 3.53 (q, 4H, 2 × CH₂), 4.45 (t, 4H, 2 × CH₂), 6.77 (d, 2H, ar), 7.37 (d, 2H, ar), 8.23 (d, 2H, ar), 8.75 (d, 2H, ar), 9.22 (t, 2H, 2 × NH, ex), 9.60 (s, 2H, ar). Anal. Calcd (C₄₅H₅₅N₁₁O₂) C, H, N.

Data for 1,9-Bis{2-[2-(dimethylamino)ethyl]-6-oxo-2,6-dihydroindazolo[3,4-*fg*]isoquinolin-5-yl}-5-methyl-1,5,9-triazanonane (10a). Yield 15%. Dimaleate mp 79–80 °C. ¹H NMR (CDCl₃) δ: 1.98 (m, 4H, 2 × CH₂), 2.25 (s, 12H, 4 × CH₃), 2.35 (s, 3H, 5-CH₃), 2.62 (t, 4H, 2 × CH₂), 2.85 (t, 4H, 2 × CH₂), 3.50 (m, 4H, 2 × CH₂), 4.50 (t, 4H, 2 × CH₂), 6.75 (d, 2H, ar), 7.32 (d, 2H, ar), 8.20 (d, 2H, ar), 8.74 (d, 2H, ar), 9.18 (t, 2H, 2 × NH, ex), 9.55 (s, 2H, ar). Anal. Calcd (C₄₁H₄₇N₁₁O₂) C, H, N.

Data for 1,9-Bis{2-[3-(dimethylamino)propyl]-6-oxo-2,6-dihydroindazolo[3,4-*fg*]isoquinolin-5-yl}-5-methyl-1,5,9-triazanonane (10b). Yield 20%. Dimaleate mp 152–153 °C. ¹H NMR (CDCl₃) δ: 1.70–1.98 (m, 4H, 2 × CH₂), 2.22 (s, 12H, 4 × CH₃), 2.29 (s, 3H, 5-CH₃), 2.40 (t, 4H, 2 × CH₂), 2.58 (t, 4H, 2 × CH₂), 3.35–3.56 (m, 8H, 4 × CH₂), 4.50 (t, 4H, 2 × CH₂), 6.78 (d, 2H, ar), 7.39 (d, 2H, ar), 8.22 (d, 2H, ar), 8.75 (d, 2H, ar), 9.22 (t, 2H, 2 × NH, ex), 9.60 (s, 2H, ar). Anal. Calcd (C₄₃H₅₁N₁₁O₂) C, H, N.

Data for 1,9-Bis{2-[2-(diethylamino)ethyl]-6-oxo-2,6-dihydroindazolo[3,4-*fg*]isoquinolin-5-yl}-5-methyl-1,5,9-triaza-

nonane (10c). Yield 30%. mp 200–201 °C. ¹H NMR (CDCl₃) δ: 0.95 (t, 12H, 4 × CH₃), 2.00 (m, 4H, 2 × CH₂), 2.38 (s, 3H, 5-CH₃), 2.43–2.60 (m, 8H, 4 × CH₂), 2.65 (t, 4H, 2 × CH₂), 2.95 (t, 4H, 2 × CH₂), 3.53 (q, 4H, 2 × CH₂), 4.44 (t, 4H, 2 × CH₂), 6.79 (d, 2H, ar), 7.38 (d, 2H, ar), 8.24 (d, 2H, ar), 8.76 (d, 2H, ar), 9.22 (t, 2H, 2 × NH, ex), 9.61 (s, 2H, ar). Anal. Calcd (C₄₅H₅₅N₁₁O₂) C, H, N.

Biophysical and Biological Evaluation. 1. Fluorescence Binding Studies. The fluorometric assays have been described previously.[17] The C_{50} values for ethidium displacement from CT-DNA and synthetic [poly(dA−dT)]₂ (AT) and [poly(dG−dC)]₂ (GC) oligonucleotides were determined using aqueous buffer (10 mM Na₂HPO₄, 10 mM NaH₂PO₄, and 1 mM EDTA at pH 7.0) containing 1.26 μM ethidium bromide and 1 μM CT-DNA, AT, and GC, respectively.[17,18]

All measurements were made in 10 mm quartz cuvettes at 20 °C using a Perkin-Elmer LS5 instrument (excitation at 546 nm and emission at 595 nm) following serial addition of aliquots of a stock drug solution [∼5 mM in dimethylsulfoxide (DMSO)]. The C_{50} values are defined as the drug concentrations that reduce the fluorescence of the DNA-bound ethidium by 50% and are calculated as the mean from three determinations.

2. In Vitro Cytotoxicity. The human colon adenocarcinoma cell line (HT29) was used for cytotoxicity testing in vitro using the SRB assay.[20] Cells were maintained as stocks in Dulbecco's modified eagle medium (DMEM) (Gibco) supplemented with 10% fetal bovine serum (Gibco) and 2 mM ʟ-glutamine (Gibco). Cell cultures were passaged twice weekly using trypsin−EDTA to detach the cells from their culture flasks. The rapidly growing cells were harvested, counted, and incubated under the appropriate concentrations (7 × 10⁵ cells/well) in 96-well microtiter plates. After incubation for 24 h, target and reference compounds dissolved in culture medium were applied to the culture wells in quadruplicate and incubated for 72 h at 37 °C in a 5% CO₂ atmosphere and 95% relative humidity. At the same time, a plate was tested to value the cell population before the drug addition (T_z). The culture fixed with cold trichloroacetic acid was stained by 0.4% SRB (Sigma-Aldrich, Milan, Italy) dissolved in 1% acetic acid. Bound stain was subsequently solubilized with 10 mM Trizma (Sigma-Aldrich, Milan, Italy), and the absorbance was read on the microplate reader Dynatech model MR 700 at a wavelength of 515 nm. The cytotoxic activity was evaluated by measuring the drug concentration resulting in a 50% reduction in the net protein increase (as measured by SRB staining) in control cells during the drug incubation (GI_{50}), the drug concentration resulting in total growth inhibition (TGI), and the drug concentration resulting in a 50% reduction in the measured protein at the end of the drug treatment as compared to that at the beginning (LC_{50}). The percentage of growth inhibition was calculated as $[(T_i − T_z)/(C − T_z)] × 100$ for concentrations for which $T_i ≥ T_z$ and as $[(T_i − T_z)/T_z] × 100$ for concentrations for which $T_i < T_z$, where T_z is the absorbance at time zero, C is the absorbance in the presence of the vehicle, and T_i is the absorbance in the presence of the drug at different concentrations. GI_{50}, TGI, and LC_{50} were obtained by interpolation on a graph of the percentage of growth versus log(M). Each quoted value represents the mean of triplicate experiments.

3. Apoptotic Assays. Apoptosis of HT-29 cells treated with the vehicle or the LC_{50} concentration of target compounds was evaluated by annexin V binding and biparametric PI/annexin V cytofluorimetric analysis.[21] To detect early stages of apoptosis, the expression of annexin V, a Ca²⁺-dependent phospholipid-binding protein with high affinity for phosphatidylserine was employed. Moreover, simultaneous staining of cells with FITC−annexin V and PI, allows for the discrimination of intact cells (annexin V⁻/PI⁻), early apoptotic cells (annexin V⁺/PI⁻), and late apoptotic or necrotic cells (annexin V⁺/PI⁺). Apoptotic cells become annexin V⁺ after nuclear condensation has started but before the cells becomes permeable to PI. Briefly, 2 × 10⁶ HT-29 cells treated with the LC_{50} of selected compounds for 6, 12, and 24 h were resuspended in 0.2 mL of binding buffer [10 mM N-2-hydroxyethylpiperazine-N′-2-ethanesulfonic acid (HEPES)/NaOH at pH 7.4,

150 mM NaCl, 5 mM KCl, 1 mM MgCl$_2$, and 1.8 mM CaCl$_2$] in the presence of 5 μL of FITC-annexin V (Bender MedSystem, Vienna, Austria) were incubated for 10 min at room temperature in the dark. The cells were washed, resuspended in 0.2 mL of binding buffer containing 10 μL of PI (20 μg/mL in PBS) (Molecular Probes, Eugene, OR), and then analyzed as mentioned above. The percentage of positive cells determined over 10 000 events was analyzed on a FACScan cytofluorimeter (Becton Dickinson, San Jose, CA) using the CellQuest software. Fluorescence intensity is expressed in arbitrary units on a logarithmic scale.

4. RT Profiler. Total RNA from HT29 cells, untreated or treated for 6 and 12 h with **1a** and **3a** (LD$_{50}$), was isolated as described above. A total of 2 μg of RNA extracted from each sample were subjected to reverse transcription in a total volume of 20 μL using the ReactionReady first strand cDNA (Superarray Bioscience Corporation). RT mixtures were incubated for 60 min at 37 °C, 5 min at 95 °C, and stored at −20 °C until the next step. For PCR array experiments, a RT^{2}Profiler Custom PCR Array (Human Apoptosis) was used to simultaneously examine the mRNA levels of 84 genes including 5 housekeeping genes in 96-well plates according to the protocol of the manufacturer (superArray BioScience). Quantitative real-time PCR was performed using a IQ5 Multicolor Real-Time PCR Detection System (BioRad, Hercules, CA) and the SuperArray's RT^2 Real-Time SYBR Green PCR Master Mix (Superarray Bioscience Corporation). Each PCR amplification consisted of heat activation for 10 min at 95 °C followed by 40 cycles of 95 °C for 15 s and 60 °C for 1 min. RNA from HT-29 cells, untreated or treated for 6 and 12 h with **7a** and **9a** (LD$_{50}$), was analyzed in triplicate, and data were normalized for β-actin levels by the $\Delta\Delta$Ct method.[22]

Supporting Information Available: Data for unknown intermediate compounds and elemental analysis results for target compounds. This material is available free of charge via the Internet at http://pubs.acs.org.

References

(1) Faulds, D.; Balfour, J. A.; Chrisp, P.; Langtry, H. D. Mitoxantrone, a review of its pharmacodynamic and pharmacokinetic properties, and therapeutic potential in the treatment of cancer. *Drugs* **1991**, *41*, 400–449.

(2) Dunn, C. J.; Goa, K. L. Mitoxantrone: A review of its pharmacological properties and use in acute nonlymphoblastic leukaemia. *Drugs Aging* **1996**, *9*, 122–147.

(3) Wiseman, L. R.; Spencer, C. M. Mitoxantrone. A review of its pharmacology and clinical efficacy in the management of hormone-resistant advanced prostate cancer. *Drugs Aging* **1997**, *10*, 473–485.

(4) Benekli, M.; Kars, A.; Guter, N. Mitoxantrone-induced bradycardia. *Ann. Intern. Med.* **1997**, *126*, 409.

(5) Krapcho, A. P.; Petry, M. E.; Getahun, Z.; Landi, J. J., Jr.; Stallman, J.; Polsenberg, J. F.; Gallagher, C. E.; Maresch, M. J.; Hacker, M. P.; Giuliani, F. C.; Beggiolin, G.; Pezzoni, G.; Menta, E.; Manzotti, C.; Oliva, A.; Spinelli, S.; Tognella, S. 6,9-Bis[(aminoalkyl)amino]benz[*g*]isoquinoline-5,10-diones. A novel class of chromophore-modified antitumor anthracene-9,10-diones: Synthesis and antitumor evaluations. *J. Med. Chem.* **1994**, *37*, 828–837.

(6) Krapcho, A. P.; Menta, E.; Oliva, A.; Di Domenico, R.; Fiocchi, L.; Maresch, M. E.; Gallagher, C. E.; Hacker, M. P.; Beggiolin, G.; Giuliani, F. C.; Pezzoni, G.; Spinelli, S. Synthesis and antitumor evaluation of 2,5-disubstituted-indazolo[4,3-*gh*]isoquinolin-6(2*H*)-ones (9-aza-anthrapyrazoles). *J. Med. Chem.* **1998**, *41*, 5429–5444.

(7) (a) Borchmann, P.; Schenell, R.; Knippertz, R.; Staak, J. O.; Camboni, G. M.; Bernareggi, A.; Hubel, K.; Staib, P.; Schulz, A.; Diehl, V.; Engert, A. Phase I study of BBR 2778, a new aza-anthracenedione, in advanced or refractory non-Hodgkin's lymphoma. *Ann. Oncol.* **2001**, *12*, 661–667. (b) Droz, J. P.; Brune, D.; Ricci, S.; Beuzeboc, P.; Chevreau, C.; Culine, S.; Flechon, A.; Camboni, M. G.; Barbieri, P.; Verdi, H. Phase II study on the activity and tolerability of BBR 3576 given to patients with advanced hormone refractory prostate cancer (HRPC). *Proc. Am. Soc. Clin. Oncol.* **2003**, *22*, 2003 (abstract 1670). (c) Borchmann, P.; Schnell, R. The role of pixantrone in the treatment of non-Hodgkin's lymphoma. *Expert Opin. Invest. Drugs* **2005**, *14*, 1055–1061. (d) Hofheinz, R. D.; Porta, C.; Hartung, G.; Santoro, A.; Hanauske, A. R.; Kutz, K.; Stern, A.; Barbieri, P.; Verdi, E.; Hehlmann, R.; Hochhaus, A. BBR 3438, a novel 9-aza-anthrapyrazole, in patients with advanced gastric cancer: A phase II study group trial of the Central European Society of Anticancer-Drug Research (CE-

SAR). *Invest. New Drugs* **2005**, *23*, 363–368. (e) Engert, A.; Herbrecht, R.; Santoro, A.; Zinzani, P. L.; Gorbatchevsky, I. EXTEND PIX301: A phase III randomized trial of pixantrone versus other chemotherapeutic agents as third-line monotherapy in patients with relapsed, aggressive non-Hodgkin's lymphoma. *Clin. Lymphoma Myeloma* **2006**, *7*, 152–154.

(8) Kobylinska, A.; Bednarek, J.; Blonski, J. Z.; Hanausek, M.; Walaskzek, Z.; Robak, T.; Kilianska, Z. M. In vitro sensitivity of B-cell chronic lymphocytic leukemia to cladribine and its combinations with mafosfamide and/or mitoxantrone. *Oncol. Rep.* **2006**, *16*, 1389–1395.

(9) Mazzanti, B.; Biagioli, T.; Adinucci, A.; Cavalletti, G.; Cavalletti, E.; Oggioni, N.; Frigo, M.; Rota, S.; Tagliabue, E.; Ballerini, C.; Massacesi, L.; Riccio, P.; Lolli, F. Effects of pixantrone on immunecell function in the course of acute rat experimental allergic encephalomyelitis. *J. Neuroimmunol.* **2005**, *168*, 111–117.

(10) (a) Villalona-Calero, M. A.; Eder, J. P.; Toppmeyer, D. L.; Allen, L. F.; Fram, R.; Velagapudi, R.; Myers, M.; Amato, A.; Kagen-Hallet, K.; Razvillas, B.; Kufe, D. W.; Von Hoff, D. D.; Rowinsky, E. K. Phase I and pharmacokinetic study of LU79553, a DNA intercalating bisnaphthalimide, in patients with solid malignancies. *J. Clin. Oncol.* **2001**, *19*, 857–869. (b) Awada, A.; Thodtmann, R.; Piccart, M. J.; Wanders, J.; Schrijvers, A. H. G. J.; Von Broen, I. M.; Hanauske, A. R. An EORTC–ECSG phase I study of LU 79553 administered every 21 or 42 days in patients with solid tumours. *Eur. J. Cancer* **2003**, *39*, 742–747.

(11) (a) O'Reilly, S.; Baker, S. D.; Sartorius, S.; Rowinsky, E. K.; Finizio, M.; Lubiniecki, G. M.; Grochow, L. B.; Gray, J. E.; Pieniaszek, H. J.; Donehower, R. C. A phase I and pharmacologic study of DMP 840 administered by 24 h infusion. *Ann. Oncol.* **1998**, *9*, 101–104. (b) Pavlov, V.; Kong Thoo Lin, P.; Rodilla, V. Cytotoxicity, DNA binding and localisation of novel bis-naphthalimidopropyl polyamine derivatives. *Chem.-Biol. Interact.* **2001**, *137*, 15–24.

(12) (a) Cholody, W. M.; Hernandez, L.; Hassner, L.; Scudiero, D. A.; Djurickovic, D. B.; Michejda, C. J. Bisimidazoacridones and related compounds: New antineoplastic agents with high selectivity against colon tumors. *J. Med. Chem.* **1995**, *38*, 3043–3052. (b) Tarasov, S. G.; Casas-Finet, J. R.; Cholody, W. M.; Kosakowska-Cholody, T.; Gryczynski, Z. K.; Michejda, C. J. Bisimidazoacridones: 2. Steady-state and time-resolved fluorescence studies of their diverse interactions with DNA. *Photochem. Photobiol.* **2003**, *78*, 313–322.

(13) Antonini, I.; Polucci, P.; Magnano, A.; Gatto, B.; Palumbo, M.; Menta, E.; Pescalli, N.; Martelli, S. Design, synthesis, and biological properties of new bis(acridine-4-carboxamides) as anticancer agents. *J. Med. Chem.* **2003**, *46*, 3109–3115.

(14) Antonini, I.; Polucci, P.; Magnano, A.; Sparapani, S.; Martelli, S. Rational design, synthesis and biological evaluation of bis(pyrimido[5,6,1-*de*]acridines) and bis(pyrazolo[3,4,5-*kl*]acridine-5-carboxamides) as new anticancer agents. *J. Med. Chem.* **2004**, *47*, 5244–5250.

(15) Krapcho, A. P.; Gallagher, C. E.; Hammach, A.; Ellis, M.; Menta, E.; Oliva, A. Synthesis of regioisomeric 6,9-(chlorofluoro)-substituted benzo[*g*]quinoline-5,10-diones, benzo[*g*]isoquinoline-5,10-diones and 6-chloro-9-fluorobenzo[*g*]quinoxaline-5,10-dione. *J. Heterocycl. Chem.* **1997**, *34*, 27–32.

(16) Krapcho, A. P.; Menta, E.; Oliva, A.; Spinelli, S. Preparation of heteroannulated indazoles as neoplasm inhibitors. International Publication Number WO 95/24407, 1995.

(17) (a) McConnaughie, A. W.; Jenkins, T. C. Novel acridine-triazenes as prototype combilexins: Synthesis, DNA binding and biological activity. *J. Med. Chem.* **1995**, *38*, 3488–3501. (b) Jenkins, T. C. Optical absorbance and fluorescence techniques for measuring DNA–drug interactions. In *Methods in Molecular Biology, Vol. 90: Drug–DNA Interaction Protocols*; Fox, K. R., Ed.; Humana Press: Totawa, NJ, 1997; Chapter 14, pp 195–218.

(18) (a) Morgan, A. R.; Lee, J. S.; Pulleyblank, D. E.; Murray, N. L.; Evans, D. H. Review: Ethidium fluorescence assays. Part 1. Physicochemical studies. *Nucleic Acids Res.* **1979**, *7*, 547–569. (b) Baguley, B. C.; Denny, W. A.; Atwell, G. J.; Cain, B. F. Potential antitumor agents. 34. Quantitative relationships between DNA binding and molecular structure for 9-anilinoacridines substituted in the anilino ring. *J. Med. Chem.* **1981**, *24*, 170–177.

(19) Bailly, C.; Pommery, N.; Houssin, R.; Hénichart, J.-P. Design, synthesis, DNA binding, and biological activity of a series of DNA minor groove-binding intercalating drugs. *J. Pharm. Sci.* **1989**, *78*, 910–917.

(20) Grever, M. R.; Schepartz, S. A.; Chabner, B. A. The National Cancer Institute–Cancer Drug Discovery and Development Program. *Semin. Oncol.* **1992**, *19*, 622–638.

(21) (a) Vermes, I.; Haanen, C.; Steffens-Nakken, H.; Reutelingsperger, C. A novel assay for apoptosis–Flow cytometric detection of phosphatidylserine expression on early apoptotic cells using fluorescein-labeled annexin-V. *J. Immunol. Methods* **1995**, *184*, 39–51. (b) Sandstrom, K.; Hakansson, L.; Lukinius, A.; Venge, P. A method to

study apoptosis in eosinophils by flow cytometry. *J. Immunol. Methods* **2000**, *240*, 55–68. (c) Antonini, I.; Santoni, G.; Lucciarini, R.; Amantini, C.; Sparapani, S.; Magnano, A. Synthesis and biological evaluation of new asymmetrical bisintercalators as potential antitumor drugs. *J. Med. Chem.* **2006**, *49*, 7198–7207.

(22) Livak, K. J.; Schmittgen, T. D. Analysis of relative gene expression data using real-time quantitative PCR and the $2^{-\Delta\Delta C_T}$ method. *Methods* **2001**, *25*, 402–408.

(23) Adams, J. M. Ways of dying: Multiple pathways to apoptosis. *Genes Dev.* **2003**, *17*, 2481–2495.

(24) Schulze-Osthoff, K.; Ferrari, D.; Los, M.; Wesselborg, S.; Peter, M. E. Apoptosis signaling by death receptors. *Eur. J. Biochem.* **1998**, *254*, 439–459.

(25) Riedl, S. J.; Salvesen, G. S. The apoptosome: Signalling platform of cell death. *Nat. Rev. Mol. Cell Biol.* **2007**, *8*, 405–413.

(26) Bradley, J. R.; Pober, J. S. Tumor necrosis factor receptor-associated factors (TRAFs). *Oncogene* **2001**, *20*, 6482–6491.

(27) Rochester, M. A.; Riedemann, J.; Hellawell, G. O.; Brewster, S. F.; Macaulay, V. M. Silencing of the IGF1R gene enhances sensitivity to DNA-damaging agents in both PTEN wild-type and mutant human prostate cancer. *Cancer Gene Ther.* **2005**, *12*, 90–100.